

LOCAL CONCRETE FAILURE UNDER BENDS OF CLOSELY SPACED REINFORCING BARS

LOKALES BETONVERSAGEN UNTER BIEGUNGEN VON ENG BEIEINANDER LIEGENDEN BEWEHRUNGSSTÄBEN

Malay Mishra, Vinay Mahadik, Jan Hofmann

Institute of Construction Materials (IWB), University of Stuttgart, Germany

SUMMARY

Rebar end anchorages with bent bars are common in RC. Although the bend offers enhanced bond resistance from bearing effects, problems may arise if the bearing forces are not resisted properly. Local failures in the concrete within the plane of the bend of hooked anchorages manifested as cover spalling can arise. Extensive studies on local failure in concrete under the bends close to concrete surface are available. In this paper the local failures for situations of closely spaced rebars is investigated. To this end a validated 3D FE modelling approach has been employed. The applicability of models developed for local failures in bend region at the edge location to situation of closely spaced rebars is investigated. Remarks on the related design approach are made relative to an alternative perspective.

ZUSAMMENFASSUNG

Bewehrungsendverankerungen mit gebogenen Stäben sind im RC-Bereich üblich. Obwohl die Biegung einen verbesserten Verbundwiderstand gegenüber den Lagerkräften bietet, entstehen Probleme, wenn den Lagerkräften nicht richtig widerstanden wird. Lokales Versagen des Betons in der Ebene der Biegung von gebogenen Verankerungen kann sich als Abplatzen der Überdeckung zeigen. Zum örtlichen Versagen im Beton unter den Biegungen in der Nähe der Betonoberfläche liegen umfangreiche Untersuchungen vor. Zu diesem Zweck wurde ein validierter 3D-FE-Modellierungsansatz angewandt und der Versagensmodus untersucht. Die Anwendbarkeit der Modelle, die für lokales Versagen im Biegebereich am Rand entwickelt wurden, wird auf Situationen mit eng beieinander liegenden Bewehrungsstäben untersucht. Es folgen Anmerkungen zu dem zugehörigen Bemessungsansatz im Vergleich zu einer alternativen Perspektive.

1. INTRODUCTION

In reinforced concrete (RC) construction, bond between concrete and steel is the basic mechanism underlying the inter-transfer forces, both compression and tension. Bending of reinforcements in the rebar end anchorage zone provide a bearing component of anchorage which further compliments the anchorage by bond action. Hence detailing practices have evolved in a way to exploit benefits from both bond as well as bearing actions. In case of bends, however, local failure of concrete under the bends can result because of the locally concentrated bearing stresses. For bent bars close to a concrete surface, the local failures typically manifest as cover spalling characterized by splitting cracks in the bend region.

The mechanism of local failure resulting from bearing stresses in bent reinforcement is comprehensively discussed in a recent study [8]. Based on extensive studies on behaviour of bends placed closed to concrete surface, a model for expressing the local concrete failures under the bend has been developed. This model has been proposed for rational design of mandrel diameter in the upcoming version of EN1992-1-1 [11].

1.1 *Local concrete failures under bent rebars*

With an objective to develop an analytical model for assessment of local concrete failure under bent rebars, Monney et.al. [8] investigated specimens with rebar bends located near a concrete edge (see Fig. 1). The effects of influencing parameters within specific ranges was investigated in the experimental program: (i) ϕ_{mand} : mandrel diameter ($4\phi \leq \phi_{mand} \leq 2.5\phi$); (ii) c : concrete cover ($0 \leq c \leq 2.5\phi$); (iii) α : bend angle ($\alpha = 45^\circ, 90^\circ \text{ and } 180^\circ$); (iv) l_{mand} : distance between multiple bends in the same plane ($0 \leq l_{mand} \leq 20\phi$); (v) ϕ : bar diameter ($\phi = 14 \text{ and } 20 \text{ mm}$); and (vi) position of the bar with respect to the casting direction (top and bottom bars). The experimental set-up and the geometry of the specimen is shown in Fig. 1.

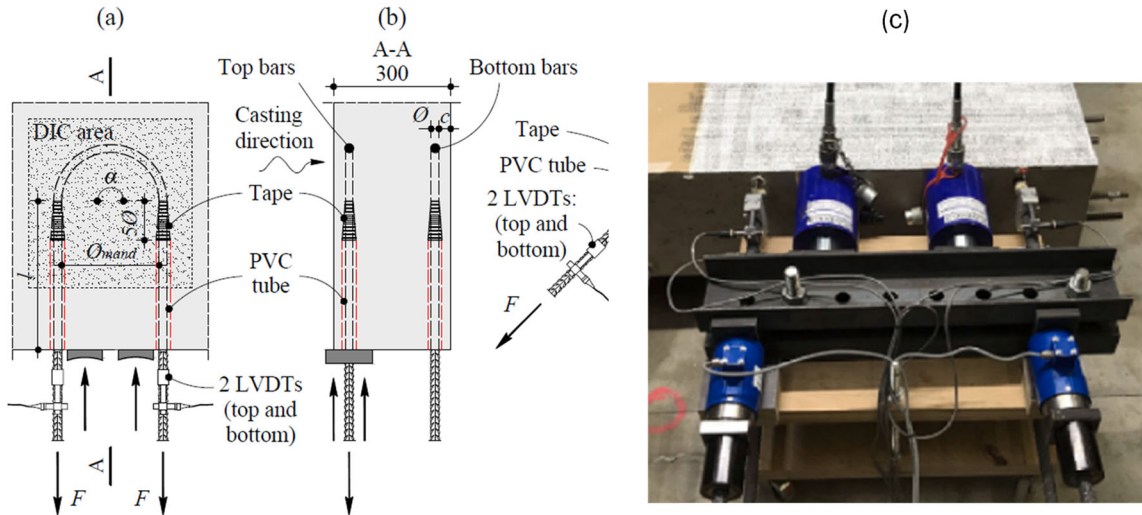


Fig. 1: Geometry of TM series specimen with U bars(a) and its cross section (b) and Experimental set-up in the laboratory (c) (source: [8])

The development of the analytical model (see (1)) was based on the failure of the confined wedge formed under the bend as shown in Fig. 2.

$$\sigma_s = \frac{2}{\pi} \cdot \frac{\phi_{mand}}{\phi} \cdot \eta_{fc} \cdot f_c + \sqrt{f_c} \cdot \left(\frac{d_{dg}}{\phi}\right)^{\frac{1}{3}} \cdot \left(\frac{c}{\phi} + \frac{1}{2}\right) \cdot \left(32 \cdot \frac{45^\circ}{\alpha^\circ} + 0.7 \cdot \frac{\phi_{mand}}{\phi}\right) \leq f_y \text{ [MPa]} \quad (1)$$

where:

σ_s is stress in reinforcement at failure (at the start of a bend) [MPa]

ϕ_{mand} is mandrel diameter [mm] and ϕ is diameter of the bar [mm]

η_{fc} is brittleness factor for concrete

f_c is concrete compressive strength measured in cylinder [MPa]

d_{dg} is parameter accounting for roughness of surfaces

c is clear concrete cover [mm]

α° is bending angle for reinforcement

f_y is yield strength of reinforcement [MPa]

It is assumed that the spalling develops due to the penetration of wedge under the bend (see Fig. 2). The tensile resistance of the concrete against the wedge creates a confinement zone. These tensile forces develop stresses which are typically larger than the uniaxial compressive strength. The wedge formation in the concrete creates a splitting crack which ultimately leads to the spalling of concrete cover. The model expression contains two terms, with the first term representing

the compression strength under tri-axial state of stress supplemented by a confinement term which considers influence of different parameters on the overall strength.

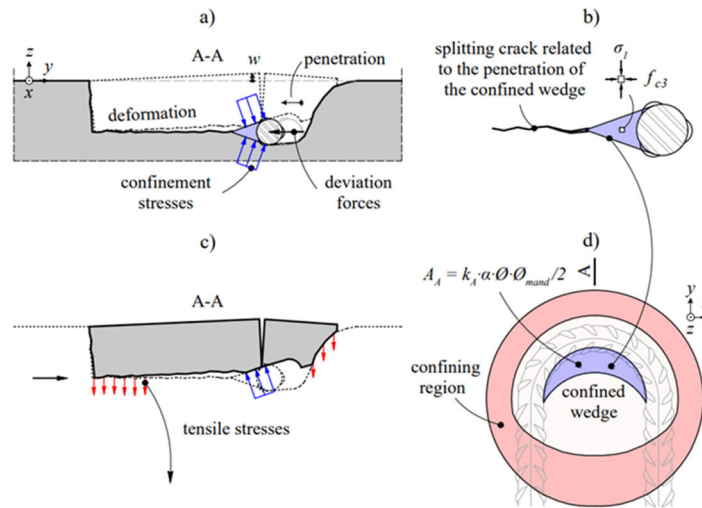


Fig. 2: Mechanism of concrete spalling (a) wedge formation and kinematics, (b) wedge shape, (c) equilibrium forces and (d) area of confinement (source: [8])

The cover to the rebar is an important parameter governing the local concrete failure and has been duly considered in the model [8]. However, since the study, focusses on rebar bends located close to edges, the cover parameter considered in the model represents minimum available radial cover to the bend region of the rebar. While adopting the model in the upcoming version of EN1992-1-1 [11], a broader definition of the cover parameter with consideration to rebar spacings has been employed. The authors could not find any data on local concrete failures in case of closely spaced rebar bends which could validate the model for such cases. This study uses finite element analysis as a tool to generate such data and tries to verify the model for situations of closely spaced rebar bends.

2. FINITE ELEMENT MODELLING AND VALIDATION

The finite element analyses are performed using MASA [10]. Concrete is modelled as solid 4-node tetrahedral elements with 3 degrees of freedom on each node. The microplane model with relaxed kinematic constraints [9] is used for definition of the constitutive law for concrete. The material properties for concrete were calculated based on the reported concrete strength using equations proposed in fib-MC-2010 [6]. Reinforcing steel is modelled using solid hexahedral elements. A von-Mises based multilinear relation was define the constitutive relation for steel.

The material properties for concrete and steel were aligned to those reported in [8]. The selected test data (both corresponding to the same geometric configuration) [8] used for validation of the finite element modelling approach is summarized in *Table 1*. The finite element model for the specimen with the boundary conditions concurrent with the test set up is shown in Fig. 3.

Table 1: Details of specimen validated from existing research (source:[8])

Specimen	α [°]	\varnothing [mm]	$\varnothing_{mand}/\varnothing$	c/\varnothing	l_{emb} [mm]	f_c [MPa]	f_{ct} [MPa]	f_y [Mpa]	F_{max} [kN]	σ_{sR} [MPa]
TM05	180	20	7	1.5	280	42.1	2.4	526	108	343
TM15	180	20	7	1.5	280	42.2	2.4	526	111	353

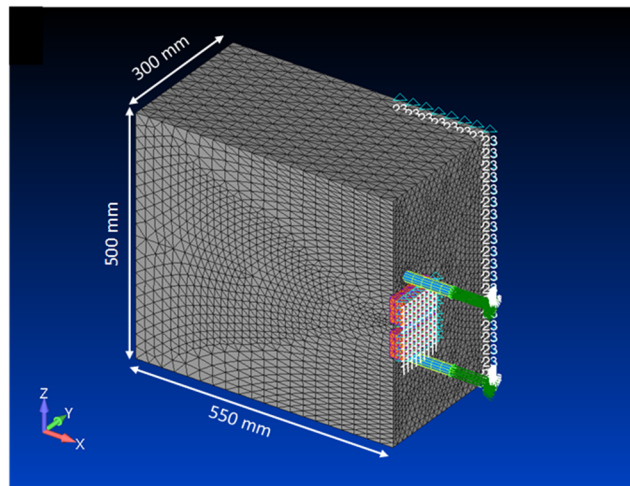


Fig. 3: Dimension of specimen TM05 selected for validation.

For the selected geometric configuration, the failure load as calculated using (1) is 116 kN in each rebar. This corresponds to a total applied load of 232 kN. The load-displacement results from analysis are compared with the test results as well as the expected value based on (1) in Fig. 4. A comparison of the observed failure mode in the experiment (TM05-15) [8] and the failure mode observed in FE simulation is shown in Fig. 5. Although the failure pattern compares reasonably well, a comparison of ultimate loads shows that the analyses provide an overestimation (FE/Test = 1.43) of the observed test result. This is probably due to the fact that the reported tensile strength of concrete mix used in the experiment rather lower than an value of uniaxial tensile strength ($f_t = 0.3f_{ck}^{2/3}$) calculated as per fib-MC-2010 [6].

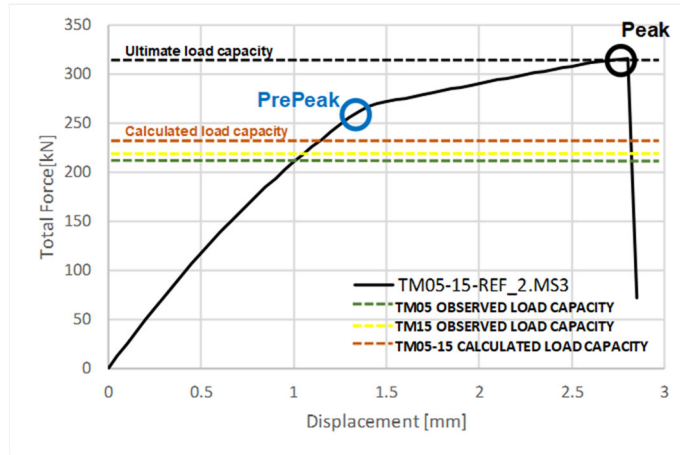


Fig. 4: Load-Displacement curve for TM05-TM15 specimen

To accommodate for the lower tensile strength corresponding to the reported compression strength, the properties of concrete are adjusted by keeping the tensile strength constant and back calculating the corresponding properties of concrete. The load displacement curve for the updated simulation is shown in Fig. 6. A reasonable comparison ($FE/Test = 1.16$) in this case is an indication that the concrete tensile strength governs the response under the local concrete failure, which is quite intuitive.

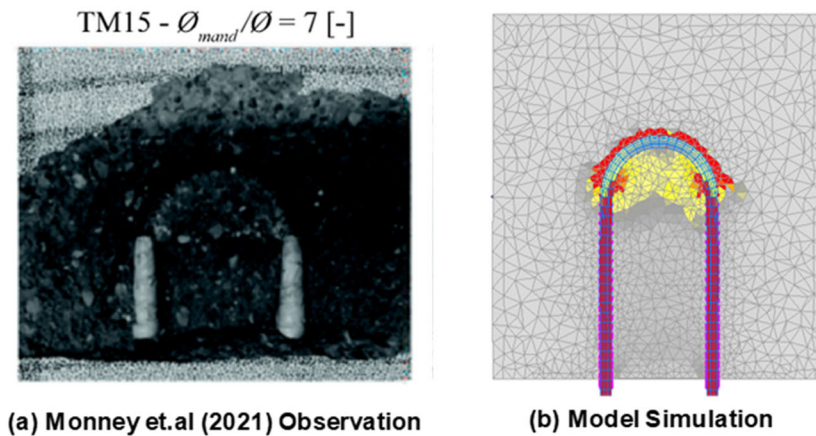


Fig. 5: Comparison of failure modes between the experiment (TM15) and the simulation (source: (a)[8])

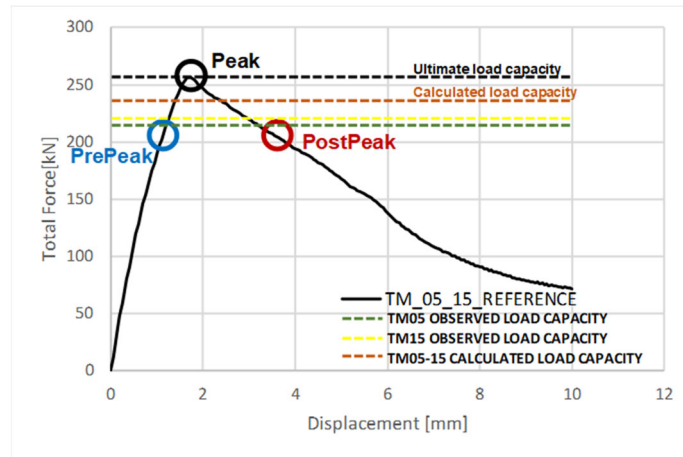


Fig. 6: Load Displacement curve for the modified simulation

3. PARAMETRIC STUDY: SPACING OF REBARS

In view of a broader definition of the cover parameter adopted in the upcoming version of EN1992-1-1 [11], it was intended to verify the applicability of the model in this regard through parametric investigation. The definition for design cover as per Monney et.al. [8] is given in equation (2). The definition adopted in the upcoming version of EN1992-1-1 [11] can be written in equation (3).

$$c_d = \min(c_x; c_y; c_z; c_{xy}) \tag{2}$$

$$c_d = \min(c_x; c_y; c_z; c_{xy}; \frac{S}{2}) \tag{3}$$

In a parametric study, three cases with closely spaced multiple bends were selected to understand the relative influence of concrete cover (c_y) and spacing (S). The parametric cases are schematically represented in Fig. 7.

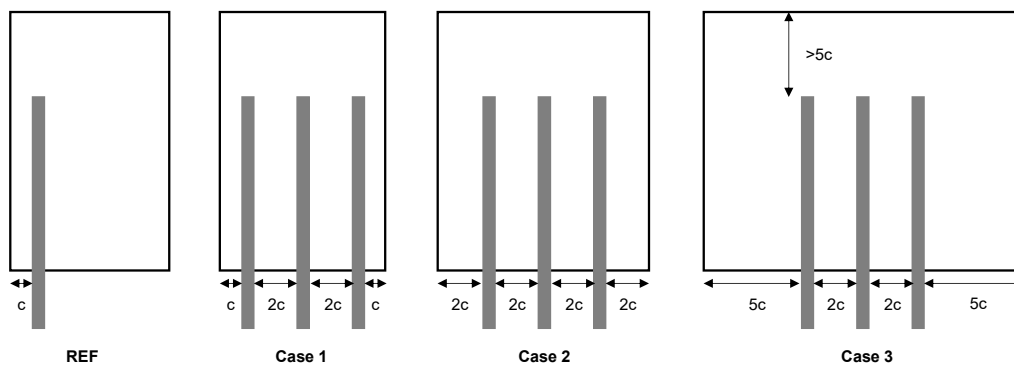


Fig. 7: Schematic representation of parametric study

Each of the cases 1, 2 and 3 were simulated using the validated FE modelling approach keeping the material properties constant throughout the models. The summary of results from simulation is listed in Table 2. To facilitate a comparison, the cover parameter calculated using (2) and (3) are also included.

Table 2: Summary of parametric simulation results

Model Name	c_d (2)	c_d (3)	Load (F_{max}) (kN)	Stress (σ_{SR}) (N/mm ²)
REF (Single rebar)	c	c	158.03	503.02
Case 1	c	c	157.97	502.83
Case 2	2c	c	157.95	502.77
Case 3	5c	c	158.17	503.47

It is observed that the load at failure does not change through the variation considered in the parametric cases. This implies, that the cover parameter c_d , which was the only parameter varied in the parametric analysis, should be the same. This verifies that it is necessary to consider the spacing within the definition of the cover parameter, which has been rightly done in the upcoming version of EN1992-1-1 [11]. The present study, nevertheless, provides a verification that the model developed for local concrete failure in near surface scenario is also applicable for situations with closely spaced rebars located far away from the concrete surfaces.

3.1 Integrating in Design Framework: Remarks

The assessment model for local concrete failures [8] under bent bars has been integrated in the upcoming version of EN1992-1-1 [11] for optimization of the bar bending details. The design requires limiting the steel stress to a limit, that the local concrete failure under the bend is precluded. Thus, local failure of concrete under the rebar bend is one possible failure of end anchorages of rebars with bends. To ascertain that this failure mode occurred in the research program [8], a confined boundary was employed in the test set up. Other failure mode like the strut failure mode at lower load are triggered when the boundary condition is changed. As shown in Fig. 8, a change in boundary conditions was investigated using FE analysis on two models: (REF and Case 1 shown in Fig. 7) were analysed. The model with single rebar showed local concrete failure under the bend

at the load level (153 kN) comparable with the case with confined boundary condition. The model with 3 rebars, however, showed in strut failure at a significantly lower load (90 kN) than that corresponding to the local concrete failure.

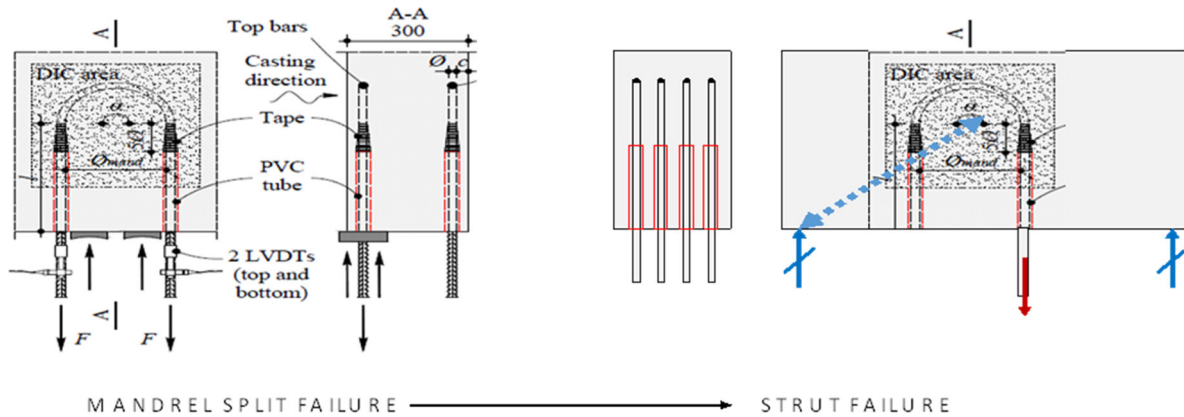


Fig. 8: Change of boundary conditions resulting in other failure modes.

It is evident from the evaluation that the boundary condition had no influence on the bearing capacity in case of single bent reinforcement, but a visible decrease (approximately 42%) in resistance of bent reinforcement was observed for multiple bent reinforcement. This is because the unconfined boundary condition triggered a shear failure before the bearing capacity for mandrel failure (spalling failure) was reached. The model discussed in (1) thus represents a specific failure mode possible for bent in rebars.

Alternative empirical models as shown in (4) have been proposed based on extensive experiments on bent rebars [3]. These models have been adopted for the design provisions in ACI-318 [1]. The empirical model can estimate the failure load under a total of five different failure modes observed in the test program.

$$T_h = 35.4 \cdot f_{cm}^{0.29} \cdot l_{eh}^{1.06} \cdot d_b^{0.54} + 37.6 \cdot \left(\frac{NA_{tr}}{n} \right)^{1.06} \cdot d_b^{0.59} \text{ [N]} \quad (4)$$

where:

T_h is anchorage strength of hooked bar [N]

f_{cm} is average concrete compressive strength [MPa]

l_{eh} is embedment length measured from outside end of hook, point of tangency, to front face of column [mm]

N, A_{tr}, n are transverse reinforcement factor. (Ignored for this case)

d_b is nominal diameter of hooked bar [mm]

To demonstrate the transition between different failure modes, the experiments 244, 245, 246 and 243 from [3] are considered (see Fig. 9). All these 4 specimens have similar configuration of anchored rebars with increasing straight anchorage length. For specimen 244 with the lowest amount of longitudinal reinforcement in column, the flexural failure of the column was observed. With an increased column longitudinal reinforcement and the low anchorage length of 254 mm, a front pull-out failure was observed for specimen 245. With further increase in the anchorage length, the failure mode transition to side blowout failure was observed. It is noted here that the side blowout failure reported by [3] is very similar to the local concrete failure under the bends manifested by cover spalling.

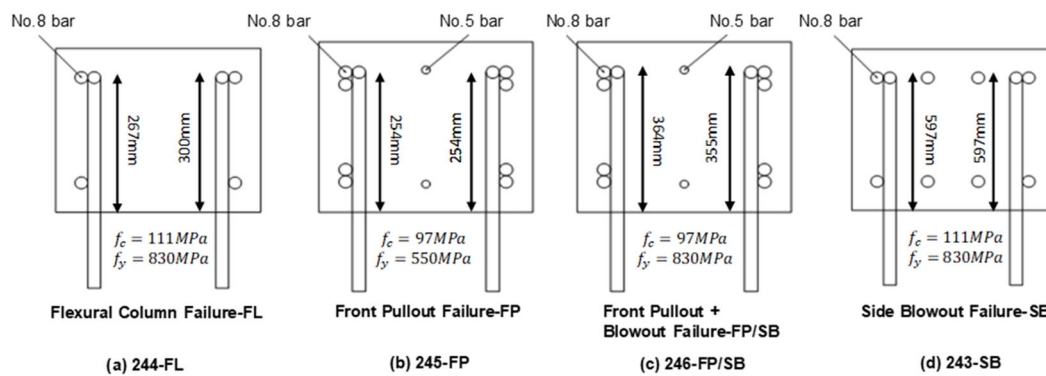


Fig. 9: Selected specimens to demonstrate transition between different failure modes [3]

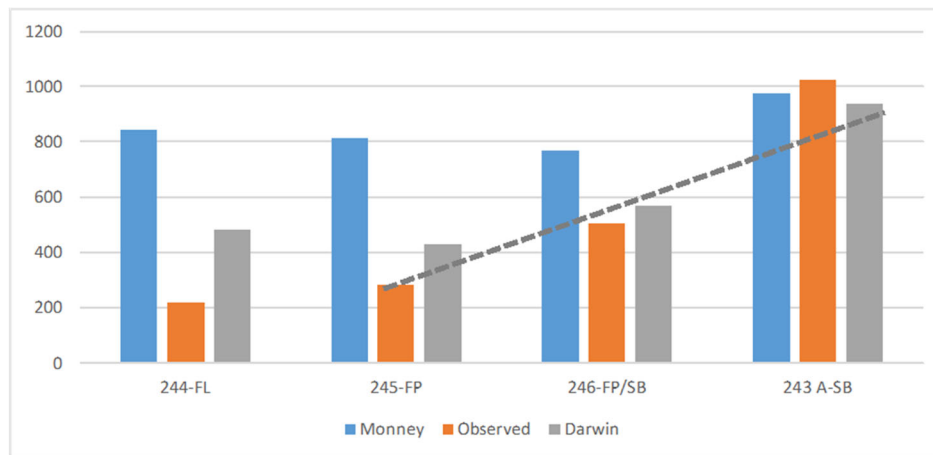


Fig. 10: Rebar force values for selected specimens

A comparison rebar forces as evaluated by (1): Monney, (4): Darwin and those observed in the tests is presented in Fig. 10. For specimen 244 with column flexure failure, both (1) as well as (4) provided rebar force values much higher than that observed in the tests. This is because column flexural failure depends on

column cross section and configuration had low reinforcement in the column section which triggered the failure at lower load level. For failure of anchorage zone (pull out or side face blowout), the empirical equation (4) is observed to provide reasonable estimate of the test results. However, the expression (1) provided comparable force estimates only in the case of side face blowout.

Thus, there are two possible approaches to design of rebar end anchorage zones. The approach in EN1992-1-1 [11] considers each of the possible failure modes in the rebar anchorage zone: pull out, splitting and local failure under the bends of the rebars using separate models. The governing failure mode for the anchorage system is evaluated based on a hierarchy of the different failure modes. The approach in ACI-318 [1] on the other hand considers only one empirical expression that is applicable for anchorage failures irrespective of the mode of failure. A more harmonious consideration of this approaches is required for an evolution of the knowledge and practical design consideration for rebar anchorage zones.

4. CONCLUSIONS

Following conclusions are drawn in the present paper:

1. The mechanics underlying the model for local concrete failure under the rebar bends [8] was discussed briefly. It was observed that the spacing of rebar was not included as an influencing parameter in the model.
2. For localized failure occurring under bearing action of the mandrel bends the FE modelling approach was successfully validated using the available experiment data.
3. Using parametric analysis, it was observed that half of the rebar spacing should be included in the definition of the cover parameter. The model for local concrete failure for rebar bends located close to concrete surface [8] was found to be applicable for situations with closely spaced rebars located away from influence of surfaces.
4. The influence of boundary conditions was studied in the FE parametric analysis. They show that in a drop in anchorage strength can occur due to the action of a separate failure mode before mandrel splitting resulting from change in the boundary condition. Mandrel theory deals with a particular failure mode and fails to accommodate for any transition in failure mode. The research from Darwin et.al [3] empirically considers the behaviour of a spe-

cific type of rebar end anchorage without any explicit consideration of different modes was also discussed. This opens the door for further investigation in this direction to identify if the design expressions in the existing codes should address an individual failure mode or a harmonized and integrated theory accounting for all the failure modes is needed.

REFERENCES

- [1] ACI-318-19: *Building code requirements for structural concrete (ACI 318-19) and commentary (ACI 318R-19)*. American Concrete Institute, p. 579, 2019
- [2] BASHANDY, T.: *Application of headed bars in concrete members*, The University of Texas at Austin, 1996
- [3] DARWIN, D. et al.: *Conventional and High-Strength Hooked Bars—Part 1 and Part 2: Anchorage Tests and Data Analysis*, 2017
- [4] DE VRIES, R.: *Application of headed reinforcement in concrete*, The University of Texas at Austin, 1996
- [5] EN:1992-4.: *Eurocode 2 - Design of concrete structures - Part 4: Design of fastenings for use in concrete*. British Standard Institutions (BSI), 2018
- [6] FIB-MC-2010.: *fib Model code for concrete structures 2010*. International Federation for Structural Concrete (fib), 2013
- [7] MAHADIK, V.: *Post installed rebar end anchorages in reinforced concrete structural connections*, 2022
- [8] MONNEY, F. et al.: *Design against splitting failures in reinforced concrete due to concentrated forces and minimum bend diameter of reinforcement*, 2021
- [9] OZBOLT, J. et al.: 'Microplane model for concrete with relaxed kinematic constraint', *International Journal of Solids and Structures*, vol. 38, no. 16, pp. 2683–2711, 2001
- [10] OZBOLT, J.: 'Masa 3: Finite element program for 3D nonlinear analysis of concrete and reinforced concrete structures', *manual*, 2010
- [11] prEN 1992-1-1: *Eurocode 2: Design of concrete structures - Part 1- 1: General rules for buildings, bridges, and civil engineering structures (DRAFT)*. European Committee for Standardization, 2021